Molecular dynamics characterization of void defects in crystalline (1,3,5-trinitro-1,3,5-triazacyclohexane)

Sylke Boyd,[1,a)] Jane S. Murray,[2] and Peter Politzer[2]
[1]*Division of Science and Mathematics, Physics Discipline, University of Minnesota, Morris, Morris, Minnesota 56267, USA*
[2]*Department of Chemistry, University of New Orleans, New Orleans, Louisiana 70148, USA and Department of Chemistry, Cleveland State University, Cleveland, Ohio 44115, USA*

(Received 16 September 2009; accepted 27 October 2009; published online 25 November 2009)

In the context of a continuing investigation of factors that affect the sensitivities of energetic materials to detonation initiation, we have carried out a molecular dynamics characterization of void defects in crystalline (1,3,5-trinitro-1,3,5-triazacyclo-hexane). An empirical force field that is capable of handling flexible molecules in a pliable crystal was used. Voids ranging in size from 2 to 30 adjacent vacated sites were created in model lattices of 216 or 512 molecules. Energetic and geometric ground state properties were determined. The void formation energy per molecule removed was found to decrease from 50 kcal/mol for a single vacancy to about 23 ± 2 kcal/mol for voids larger than one unit cell (8 molecules). Analysis of the local binding energies in the vicinity of a void reveals not only the expected decrease for molecules directly on the void surface but also a wide spread of values in the first 5–10 Å away from the surface; this includes some molecules with local binding energies significantly higher than in the defect-free lattice. Molecular conformational changes and reorientations begin to be found in the vicinities of voids larger than one unit cell. Thermal behavior investigated includes void and molecular diffusion coefficients and fluctuations in void size. © *2009 American Institute of Physics*. [doi:10.1063/1.3265986]

I. BACKGROUND

The mechanisms of detonation initiation in energetic materials continue to be a challenging area of inquiry. Its importance lies not only in the need to achieve a more fundamental understanding of the processes that are involved but also in the safety aspect. Diminishing the sensitivities of energetic materials to detonation due to accidental stimuli—impact, shock, electric spark, etc.—is a major international objective, as reflected, for example, in the establishment by the North Atlantic Treaty Organization of the Munitions Safety Information and Analysis Center.[1]

The initiation of detonation in energetic compounds is governed by a number of factors: chemical composition, molecular and crystal structure, physical state, and the nature of the stimulus.[2–8] However a key role is generally attributed to the presence of lattice defects—vacancies, interstitial occupancies, voids, misalignments, edge and screw dislocations, etc. It is believed that they cause disporportionate localizations, in their immediate neighborhoods, of energy introduced by external stimuli (e.g., impact or shock).[2,3,6,9–17] These are called "hot spots." Their development in conjunction with lattice defects has been observed in molecular dynamics simulations.[12,13] It may be that this energy localization is a means of reducing defect-induced strain in the lattice, by permitting relaxation or rearrangement. Data concerning the dimensions, temperatures, and durations of hot spots are given elsewhere.[6,15,17]

How does the formation of hot spots lead to detonation? One hypothesis, which has received considerable attention, involves vibrational energy transfer and "up-pumping."[7,18–22] Hot spot energy in lattice vibrations (phonons) and low-lying "doorway" molecular modes, through anharmonic coupling, undergoes multiphonon up-pumping into the higher vibrational levels that can lead to bond-breaking, followed by subsequent exothermic reactions and detonation. It has been shown, for groups of energetic compounds, which higher rates of this vibrational energy transfer do correspond to greater sensitivities.[20–22]

Another possible explanation of how hot spots, in conjunction with void and vacancy defects, may lead to detonation initiation comes out of a computational study by Kuklja of the prominent nitramine explosive [(1,3,5-trinitro-1,3,5-triazacyclohexane, 1) (RDX)].[23] It was found that the energy required to break an $N-NO_2$ bond in an RDX molecule near a free surface of the crystal is significantly less than when it is in the bulk crystal. Since $N-NO_2$ cleavage is viewed as a possible key step in nitramine initiation, the void/vacancy-induced weakening of this bond in proximity to hot spot energy could promote detonation. Note that this interpretation and vibrational energy transfer are not mutually exclusive.

1, RDX

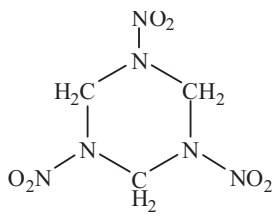

As part of a long-term computational analysis of detona-

a)Electronic mail: sboyd@morris.umn.edu.

tion initiation in energetic compounds, we have earlier developed an empirical force field for molecular dynamics/Monte Carlo simulations of crystals composed of relatively large but flexible molecules.[24] We tested our model for RDX, 1. Our procedure was successful in stabilizing the correct molecular conformer and lattice structure of (defect-free) α-RDX and in maintaining these over an extended time period and a range of temperatures and pressure conditions. Various molecular and crystal properties were satisfactorily reproduced.

A more recent molecular dynamics study, using the same model, was designed to identify vibrational modes that couple lattice and molecular degrees of freedom.[25] These could serve as doorway modes for the up-pumping of hot spot energy to high vibrational levels that can lead to bond stretching and rupture. A projection technique was applied to ascertain which normal modes of the crystal significantly engage both internal and lattice degrees of freedom. It was concluded that the most likely doorway modes are in two regions, 186–220 and 420–434 cm^{-1}.[25] Those in the first region involve center-of-mass translations, ring rotations, and NO_2 rocking, swaying and twisting. The 420–434 cm^{-1} modes again include center-of-mass translations, along with CH_2 wagging and CNCH torsion that affects NO_2 wagging.

The objective of the present work has been to characterize voids in crystalline α-RDX, as a specific kind of lattice defect and to determine their effects upon the surrounding lattice. The voids range in size from 2 to 30 adjacent empty lattice sites.

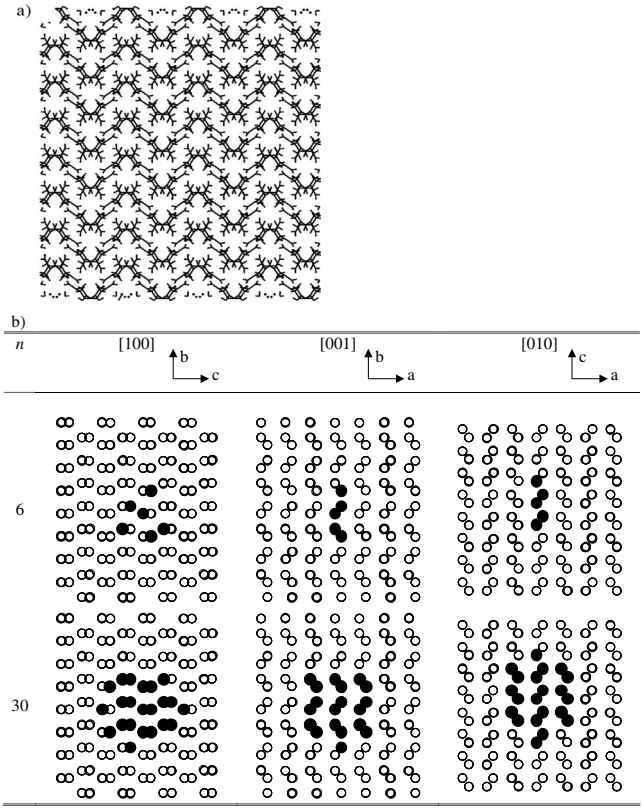

FIG. 1. (a) [001] view of the defect-free large system. (b) Sketches of void systems $n=6$ and 30, showing different lattice planes. Circles mark the center-of-mass positions of molecules, black circles mark the equilibrium positions of removed molecules.

II. COMPUTATIONAL APPROACH

Our free field and molecular dynamics procedure are discussed in detail by Boyd *et al.*[24] Bond stretching is described with a Morse potential, and angle bending with a harmonic approximation. Torsion is represented by a truncated cosine series. Nonbonded interactions are treated coulombically (intermolecular) and also with Buckingham potentials[26] (both inter- and intramolecular); long-range cutoffs of 15 Å are imposed. Parametrization was primarily with literature values for the intramolecular terms and by fitting to experimental RDX crystal data for the intermolecular ones. All molecular dynamics simulations are based on an Andersen–Berendsen scheme,[27] allowing sampling at constant pressure and temperature. Geometry optimizations were performed with a conjugate gradient procedure. Our model yields satisfactory results for a variety of molecular and crystal properties, including several that had not been involved in the fitting.[24]

Depending upon the size of the void, we used simulation cells consisting of $3\times3\times3$ or $4\times4\times4$ unit cells; we will refer to these as the smaller and the larger systems. Since there are eight RDX molecules per unit cell, the smaller defect-free system includes 216 molecules and 4536 atoms, while the larger has 512 molecules and 10 752 atoms. A view of the latter is shown in Fig. 1(a). The use of the larger system permits accommodating bigger voids while avoiding interference with the periodic boundary conditions imposed in all directions.

Cohesive voids were introduced by removing molecules, first one and then its neighbors over an increasing distance to create systems with voids of sizes from $n=1$ to $n=30$, where n is the number of vacated lattice sites. An $n=30$ void corresponds to a significant disturbance of the crystal geometry, equivalent to the removal of more than three unit cells. Two of the voids are illustrated in Fig. 1(b). Note that it shows only the surroundings of the respective voids, not the whole model lattice.

The ground states of these void systems were attained in two phases. First, stepwise simulated annealing quenched the system from an initial 250 to 10 K at a pressure of 1 atm over a total time of 500 ps. This allowed the lattice parameters to adjust to the internal stress distribution, modified by the presence of the void, and the molecules to relax around the void. The quenching was followed by geometry optimization into the ground state, which was then analyzed for its energetic and geometric features. In addition, NPT molecular dynamics trajectories were sampled for different properties; each trajectory was preceded by an equilibration to the desired thermal conditions.

The experimentally determined conformation of the RDX molecule in the crystal is *Caae*.[28,29] This designation indicates that the ring is in the chair form (C) and that two of the nitro groups are axial (a) and one equatorial (e). The ring could also have a boat (B) or a twist (T) conformation. The ring conformation is sampled using the box product of the ring diagonals, while the nitro orientations are sampled as

axial or equatorial utilizing the angle formed between the ring normal and the N–N bond as described earlier.[24] For the isolated molecule, we have found the *Caaa* and *Caae* conformers to have essentially the same energy,[24] which is consistent with other studies.[30,31] The intramolecular energy of our *Caae* conformer is about 1 kcal/mol higher in the lattice than as an isolated molecule, due to small differences in NO_2 wag and torsional angles.

III. RESULTS AND DISCUSSION

A. Energetic analysis of voids

We define the formation energy of a void defect of size n as

$$E_f(n) = E_{syst}(n) + nE_{mol} - E_{syst}(0), \quad (1)$$

in which $E_{syst}(n)$ is the ground state energy of the system with a void of size n, E_{mol} is the energy of an isolated relaxed *Caae* conformer, and $E_{syst}(0)$ is for the ideal crystal without a void. $E_f(n)$ represents the energy required to remove and separate n molecules, taking into account the subsequent relaxation of the surrounding lattice; this can include conformational changes in the molecules bordering the void, and rotations and center-of-mass translations in response to the change in the stress field.

Earlier,[24] we found the formation energy $E_f(1)$ of a single vacancy to be 51 kcal/mol, within the limitations of a fixed box size. With flexible box boundaries, $E_f(1)$ now decreases to 50 kcal/mole. This is in good agreement with the 55 kcal/mol coming out of the work of Kuklja and Kunz,[32] which includes molecular but not lattice relaxation.

The total formation energies of the voids that we considered are presented in Fig. 2(a); the formation energies per molecule removed, $E_f(n)/n$, are in Fig. 2(b). For some intermediate void sizes, we calculated these quantities for both the small and the large systems, to verify that the values are consistent within the given boundary conditions. Slight discrepancies between the small and the large systems reflect differences in the choices of the vacated sites rather than problems of boundary conditions.

Figure 2(b) shows that the void formation energy per molecule removed initially decreases rapidly with increasing void size, since each newly removed molecule had fewer neighbors than did the preceding one and was therefore significantly less tightly held. However the effect of this soon levels off, and $E_f(n)/n$ approaches a value that is approximately half of the formation energy of a single vacancy. This occurs after void size $n=8$, which corresponds to one vacated unit cell. A linear fit of $E_f(n)$ versus n, Fig. 2(a), has a slope of 23 ± 2 kcal/mol per additional molecule removed, which is in accord with $E_f(n)/n$ for larger voids, Fig. 2(b).

The changes in lattice parameters accompanying void formation, during the initial thermalization, were less than 0.3% over the entire range of void sizes. The largest was a decrease of 0.29% in a for $n=30$. The density of the system decreased from 1.91 g/cm^3 for the ideal, defect-free lattice to 1.81 g/cm^3 for $n=30$. The latter should be more realistic, and indeed the experimental density is 1.806 g/cm^3.[28]

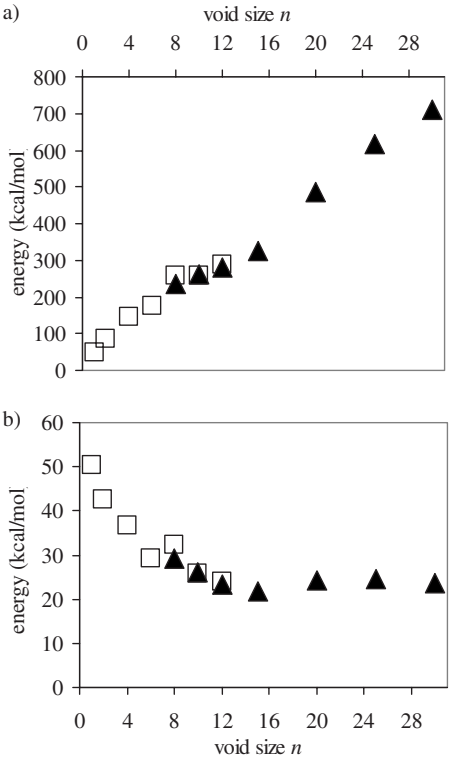

FIG. 2. (a) Total formation energy of the void vs size of the void. Squares are results of calculations for the smaller system, triangles are for the larger system. (b) Formation energy of the void per removed molecule vs size of the void. Squares are results of calculations for the smaller system, triangles are for the larger system.

Two other energetic quantities of interest are the average binding energy per molecule and the various local binding energies. The average binding energy per molecule, $\bar{E}_b(n)$ for a system with void size n, is that needed to separate the lattice into isolated molecules. It is given by

$$\bar{E}_b(n) = \frac{[(N-n)E_{mol} - E_{syst}(n)]}{N-n}, \quad (2)$$

where N is the number of molecules in the absence of any vacancies, either 216 or 512. Since the largest voids that we have investigated represent less than 6% of the molecules in either lattice, their effects upon $\bar{E}_b(n)$ are negligible, and it is between 27 and 28 kcal/mol for all of the systems considered, $n=0$ to $n=30$. This is in reasonable agreement with the experimental enthalpy of sublimation of RDX that was one of the fitting criteria for our force field,[24] 31.1 kcal/mol;[33] a more recent experimental value, is 26.8 kcal/mol.[34]

The local binding energy at a specific lattice site x, $E_b(n,x)$, is what is required to remove a molecule from that site. We obtain $E_b(n,x)$ from the intermolecular interactions portion of our force field, which consists of Coulomb and van der Waals (vdW) terms;[24] it does not include any conformational relaxation

$$E_b(n,x) = E_{inter}(n,x) - E_{inter}(n). \quad (3)$$

In Eq. (3), $E_{inter}(n)$ and $E_{inter}(n,x)$ are the intermolecular interaction energies in the system with void size n and the same system with an additional molecule removed at site x.

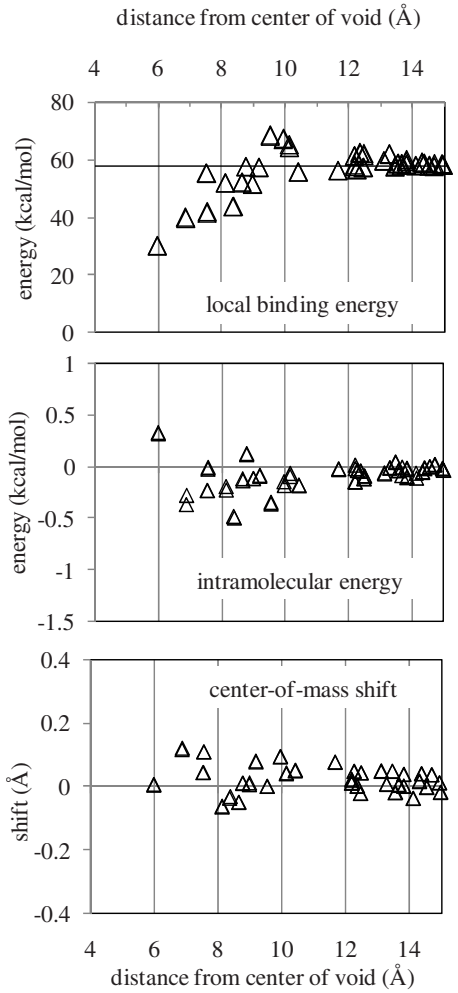

FIG. 3. Ground-state local binding energy per molecule, intramolecular energy, and center-of-mass shift at increasing distances from the center of the void $n=2$. The horizontal line at 58 kcal/mol in the top plot represents the local binding energy per molecule in the ideal defect-free lattice. A negative center-of-mass shift is toward the center of the void.

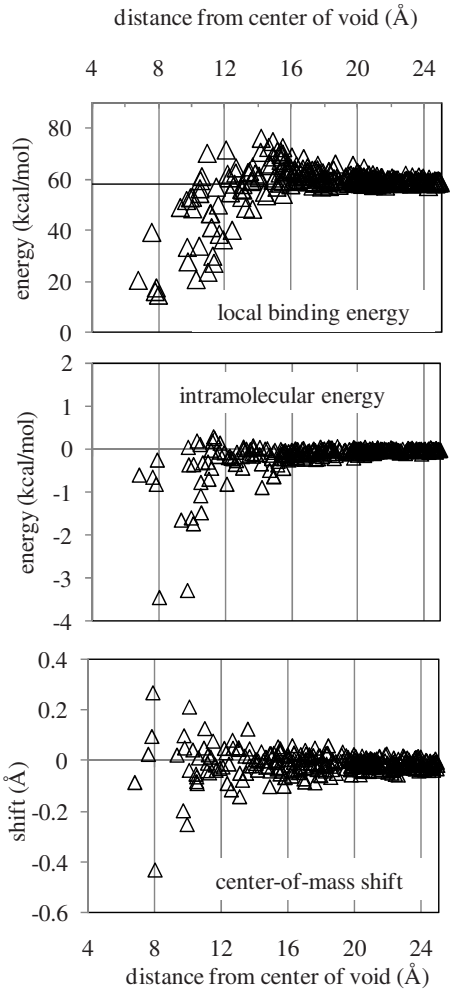

FIG. 4. Ground-state local binding energy per molecule, intramolecular energy, and center-of-mass shift at increasing distances from the center of the void $n=10$, large system. The horizontal line at 58 kcal/mol in the top plot represents the local binding energy per molecule in the ideal defect-free lattice. A negative center-of-mass shift is toward the center of the void.

For a molecule in the ideal defect-free lattice, this local binding energy $E_b(0,x)$ is 58 kcal/mol. This differs from the formation energy of a single vacancy, given earlier as $E_f(1)=50$ kcal/mol, because conformational and lattice relaxations in the surroundings of the vacancy are taken into account in the formation energy but not in the local binding energy.

Since the voids tend to have irregular shapes and there is also some shifting of molecules during geometry optimization, $E_b(n,x)$ varies with angular position around a void. The top panels of Figs. 3–5 show the local binding energies at different distances from the centers of voids with $n=2$, 10, and 30, which are representative, respectively, of what is observed for the other small, intermediate and large voids investigated. Molecules located at or near the surface of a void are interacting with fewer neighbors and are therefore less tightly held in the lattice; $E_b(n,x)$ can be as low as 10 kcal/mol (Figs. 4 and 5) compared to 58 kcal/mol in the defect-free lattice. As the distance from the center of the void increases, a large spread in local binding energies is seen for the first few angstroms, especially for the larger voids, for which $E_b(n,x)$ ranges between 20 and 85 kcal/mol. Finally, at yet longer distances, the local binding energies do approach their defect-free value of 58 kcal/mol.

In seeking to identify the factors that influence local binding energies in the vicinities of voids, we looked initially at (a) molecular conformational changes and (b) shifts in molecular centers-of-mass. Both of these affect the relative orientations and separations of molecules, and thus the intermolecular interaction energies.

Conformational changes are reflected in the intramolecular energies, which comprise contributions from bond stretching, angle bending, torsions and internal nonbonded interactions.[24] The middle panels of Figs. 3–5 show the intramolecular energies of molecules at various distances from the void centers; the energies are relative to that of a molecule in the ideal defect-free lattice. The negative values in the vicinity of each void indicate that these molecules are less strained than those in the bulk lattice, perhaps due to having fewer neighbors and more space. The changes are primarily in bending and torsional energies with a slight contribution from intramolecular nonbonding interactions. However the effects upon intramolecular energies are an order of

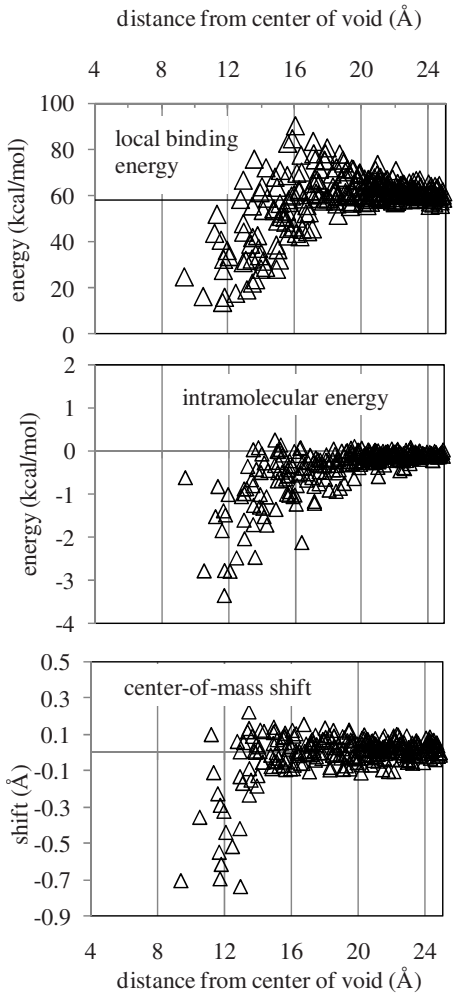

FIG. 5. Ground-state local binding energy per molecule, intramolecular energy, and center-of-mass shift at increasing distances from the center of the void $n=30$, large system. The horizontal line at 58 kcal/mol in the top plot represents the local binding energy per molecule in the ideal defect-free lattice. A negative center-of-mass shift is toward the center of the void.

magnitude smaller than the observed fluctuations in local binding energies and cannot account for the spread in these.

A useful perspective can be obtained by looking separately at the two components of the intermolecular interaction energies, the vdW and the coulomb. The former, represented by a Buckingham potential, are negative (attractive) and dominate at short intermolecular separations but they decay rapidly, as 1/r (Ref. 6). The coulomb is positive (repulsive) because the shortest intermolecular distances are usually between negative NO_2 oxygens. They fall off more slowly, as 1/r. The vdW and Coulomb contributions to the local binding energies $E_b(n,x)$ reflect these behaviors but with the opposite signs, due to Eq. (3). This can be seen in Fig. 6 for void sizes $n=2$, 10, and 30. Stochastic scattering of these values is due to variations in local conditions at each molecule's lattice site.

In the absence of a void, or far away from it, a molecule's pair interactions are the same in all directions due to the symmetry of the lattice. The net force upon it is zero and the local binding energy $E_b(n,x)$ is constant at about 58 kcal/mol. For molecules near a void, however, their interactions with others in their vicinities are anisotropic, leading to

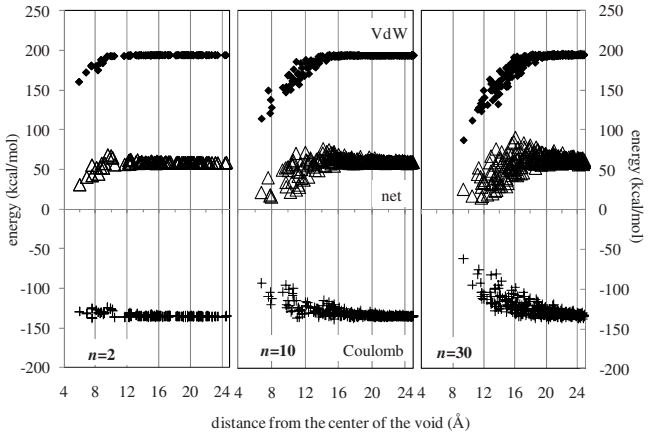

FIG. 6. Components of local binding energy at increasing distances from the centers of voids $n=2$, 10 and 30. vdW contributions, Coulomb, and net intermolecular interactions are shown.

variations in numbers and strengths of interactions as well as possible conformational changes. The observed spread of local binding energies in the region around the void can be attributed to such ensemble effects.

The differing decay rates cause the overall intermolecular interaction energy to pass through an effective maximum at some distance from the void. Molecules located before this maximum experience, on the average, a force drawing them into the void; molecules beyond the maximum feel a smaller net force directed away from the void. The lower panels of Figs. 3–5 indicate that the greatest center-of-mass shifts during initial relaxation occur in close proximity to the voids. For void $n=10$, for example, they are within 8–10 Å of its center. The shifts are greatest for the larger voids, as much as 0.7 Å for size $n=30$, and the molecules exhibit a strong preference for relaxing toward the center of the void. There is significant statistical scattering in the binding energies and in the center-of-mass shifts, owing to individual conformational states, positions in the lattice, distances from the void surface and similar factors.

Ring and NO_2 conformational changes and ring orientations reduce molecular strain near the voids in the ground state. For void sizes $n<8$, the *Caae* conformation is generally maintained at all distances, with some variations in $N-NO_2$ alignments that account for the small decreases observed in intramolecular energy (Fig. 3). With intermediate size voids, there are likely to be a few ring and NO_2 conformational changes and sizeable reorientations, especially near the voids. For example, near the $n=10$ void is a *Caaa* conformer which deviates by 60° from its original ring orientation. A second molecule has a nonchair conformation. With large voids are associated a significant number of conformations other than *Caae*, as well as reorientations (Fig. 7). These effects can extend into the region in which the maximum local binding energies are observed, beyond which the system eases into the defect-free crystal structure.

B. Thermal behavior of voids

We subjected systems with differently sized voids to 80 ps molecular dynamics simulations, at a pressure of 1 atm and temperatures of 300 and 400 K. We define the radius of

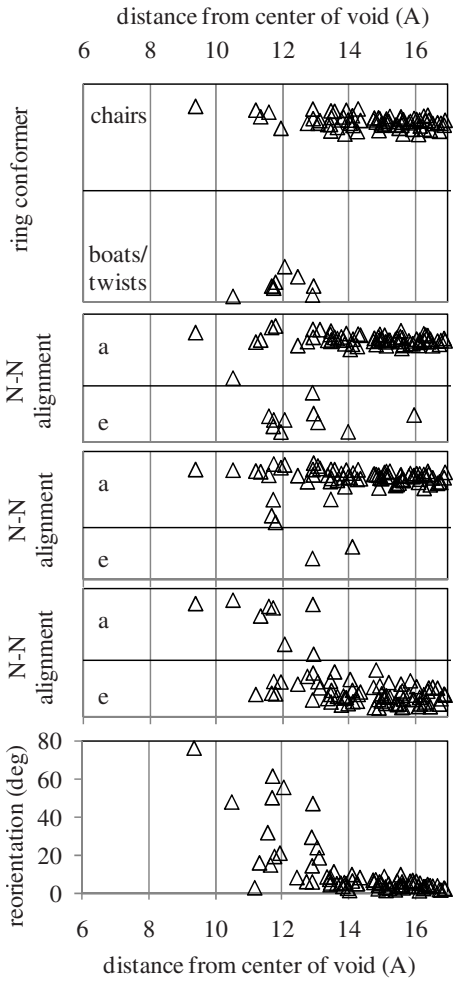

FIG. 7. Molecular conformers at increasing distances from center of void $n=30$, large system. Top panel: ring conformations; middle three panels: $N-NO_2$ alignments with respect to ring normal vectors (a=axial, e=equatorial); bottom panel: reorientation angles of the ring normal vectors.

a void as that of the largest sphere that can fit within it, as limited by either (a) the nearest molecular center-of-mass or (b) the next-nearest atom. The first definition gives the larger radii, by somewhat more than 2 Å.

There is a small decrease in void radius with temperature for larger voids ($n \geq 10$), caused by boundary molecules migrating into the void. Thermal fluctuations in void radii increase if the void size exceeds $n=10$. Plots of void radius versus time at 400 K are in Fig. 8 for void sizes $n=8$ and $n=20$. Note that diffusion into the $n=20$ void occurs after about 46 ps, leading to a decrease in its radius.

The diffusion coefficient of a void can be determined from the change in position of its center with time, using the Einstein relationship

$$D = \lim_{x \to \infty} \frac{1}{6t} \langle l^2(t) \rangle. \tag{4}$$

The mean square displacement length,

$$\langle l^2(t) \rangle = \frac{1}{t} \int_a^{a+t} [l(t')]^2 dt', \tag{5}$$

is sampled over the complete time series by shifting the sample interval t over the whole 80 ps trajectory. Figure 9

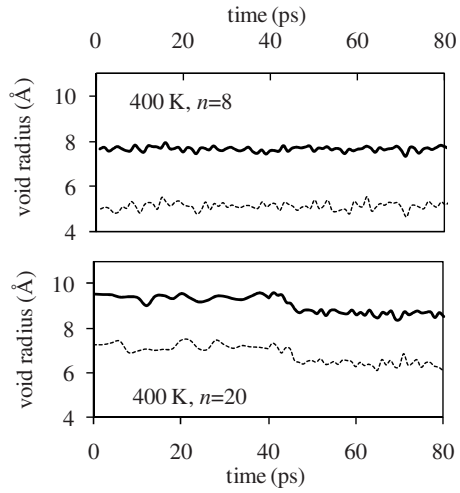

FIG. 8. Void radius vs time for the $n=8$ and $n=20$ voids at 400 K, 1 atm, large system. The darker plots are for the radii defined with respect to nearest molecular center-of-mass; the lighter ones are for radii relative to next-nearest atom.

shows a few examples of the mean square displacement length of the void center versus time. There are fewer data points for the long terms than for the short ones, resulting in larger fluctuations for the former. From these data can be estimated the diffusion coefficients of the centers of the voids. These are of the order of magnitude of 10^{-11} to 10^{-10} m^2/s. The void centers migrate by mechanisms that involve individual molecules shifting along the inner void surface.

In Fig. 10, the individual molecular diffusion coefficients at 400 K for void size $n=20$ are shown as a function of radial distance from the void center. The highest diffusion coefficient is observed for the innermost molecule, at $(4.2 \pm 0.7) \times 10^{-10}$ m^2/s. In contrast, the value for the void center itself is $(1.1 \pm 0.3) \times 10^{-10}$ m^2/s. Both are significantly above the baseline molecular diffusion coefficient of the order of 10^{-12} m^2/s that is observed for a molecule in the defect-free lattice, which is restricted to thermal fluctuations around its equilibrium site. During the 80 ps sampling period, one of the innermost molecules moved a distance of more than 4.5 Å, which included one actual fast diffusion step, to a new equilibrium site. At 300 and 400 K, all of the molecules exhibit active side group fluctuations, including transitions

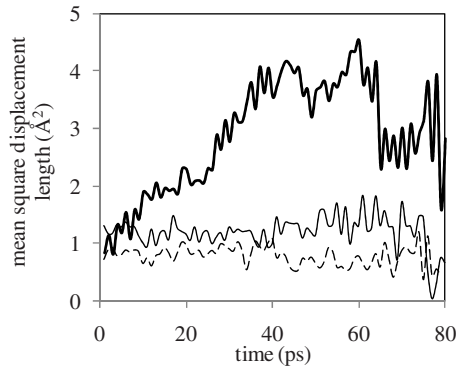

FIG. 9. Time dependence of mean square of the displacement length $\langle l^2(t) \rangle$ of the void center. Solid bold plot is for void $n=20$ at 400 K; solid plot is for $n=8$ at 400 K and dashed plot is for $n=8$ at 300 K.

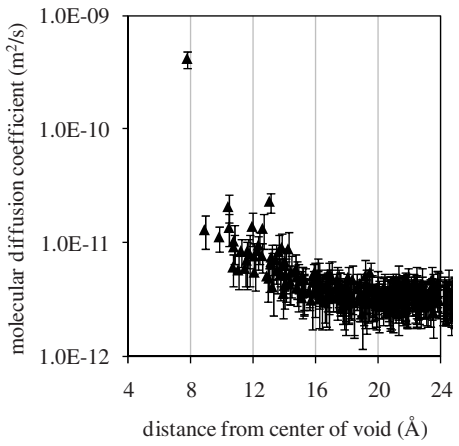

FIG. 10. Molecular diffusion coefficient for $n=20$ at 400 K as a function of distance from the center of the void. Statistical fluctuations are indicated by error bars.

between axial and equatorial NO_2 positions. It is common to find *Caaa* conformers in the vicinity of the void, as well as molecules going between twist and chair conformations.

IV. SUMMARY

For two of the global ground state properties of RDX that we have examined, the effects of the voids up to $n=30$ are minimal. The lattice parameters of the systems and the average binding energy per molecule remain essentially the same for all of the voids as for the defect-free lattice. However the density decreases from 1.91 to 1.81 g/cm^3. Other global properties, such as the band gap,[32,35,36] are also expected to be affected.

The formation energy per molecule removed that is required to produce a void of n vacated sites is 50 kcal/mole for $n=1$, but decreases rapidly up to $n=8$ since the removal of each one results, at that point, in a significant weakening of the net attractive forces felt by its neighbors. This begins to be less important after $n=8$, and by $n=12$, the energy required per molecule has leveled off to about 23 ± 2 kcal/mole.

Our particular interest is in what happens on a molecular level in the vicinities of the voids. The local molecular binding energies at or near the surface of a void are considerably less than in the bulk lattice, and this continues for several angstroms away from the void. At about 5–10 Å from the surfaces of the intermediate and larger voids, there is a considerable spread in local binding energies, with some exceeding the bulk value. This region also sees significant changes in molecular conformations: chair to boat or twist, axial NO_2 to equatorial and the reverse, and reorientations of the ring normal vectors. The intramolecular energies are more negative than in the bulk, suggesting diminished strain. In addition, there is translational movement of these molecules, both into and away from the void, during the geometry optimization.

The diffusion mobilities of individual molecules on the void surface are four times that of the void center. For a large void, molecules immediately adjacent to it exhibit strong conformational fluctuations and often have *Caaa* conformations.

Overall, the picture is one of considerable activity, at the surface of a void and extending for several angstroms away from it. The next phase of this investigation shall focus upon how this may affect lattice to molecular-mode transfer of vibrational energy.

ACKNOWLEDGMENTS

We appreciate the funding provided by the Defense Threat Reduction Agency Contract No. HDTRA1-07-1-0002, Project Officer Dr. William Wilson. S.B. acknowledges the support of the Minnesota Supercomputing Institute at the University of Minnesota.

[1] http://hq.nato.int/related/nimic.
[2] M. J. Kamlet, 6th Symp. (Internat.) Deton., Report No. ACR 221, Office of Naval Research, 321 (1976).
[3] M. J. Kamlet and H. G. Adolph, Propellants, Explos., Pyrotch. **4**, 30 (1979).
[4] S. Iyer and N. Slagg, in *Structure and Reactivity*, edited by J. F. Liebman and A. Greenberg (VCH, New York, 1988), Chap. 7.
[5] T. B. Brill and K. James, Chem. Rev. **93**, 2667 (1993).
[6] P. Politzer and J. S. Murray, in *Energetic Materials, Part 2. Detonation, Combustion*, edited by P. Politzer and J. S. Murray (Elsevier, Amsterdam, 2003), Chap. 1.
[7] D. D. Dlott, in *Energetic Materials, Part 2. Detonation, Combustion*, edited by P. Politzer and J. S. Murray (Elsevier, Amsterdam, 2003), Chap. 6.
[8] S. A. Schackelford, Central Europ. J. Energ. Mater. **5**, 75 (2008).
[9] F. P. Bowden and A. D. Yoffe, *Fast Reactions in Solids* (Butterworths, London, 1958).
[10] A. W. Campbell, W. C. Davis, J. B. Ramsay, and J. R. Travis, Phys. Fluids **4**, 511 (1961).
[11] R. W. Armstrong, C. S. Coffey, V. F. DeVost, and W. L. Elban, J. Appl. Phys. **68**, 979 (1990).
[12] D. H. Tsai and R. W. Armstrong, J. Phys. Chem. **98**, 10997 (1994).
[13] J. W. Mintmire, D. H. Robertson, and C. T. White, Phys. Rev. B **49**, 14859 (1994).
[14] J. Sharma, C. S. Coffey, A. L. Ramaswamy, and R. W. Armstrong, Mater. Res. Soc. Symp. Proc. **418**, 257 (1996).
[15] C. M. Tarver, S. K. Chidester, and A. L. Nichols III, J. Phys. Chem. **100**, 5794 (1996).
[16] M. M. Kuklja, Appl. Phys. A: Mater. Sci. Process. **76**, 359 (2003).
[17] P. Politzer and S. Boyd, Struct. Chem. **13**, 105 (2002).
[18] A. Tokmakoff, M. D. Fayer, and D. D. Dlott, J. Phys. Chem. **97**, 1901 (1993).
[19] S. Chen, W. A. Tolbert, and D. D. Dlott, J. Phys. Chem. **98**, 7759 (1994).
[20] L. E. Fried and A. J. Ruggiero, J. Phys. Chem. **98**, 9786 (1994).
[21] K. L. McNesby and C. S. Coffey, J. Phys. Chem. B **101**, 3097 (1997).
[22] S. Ye, K. Tonokura, and M. Koshi, J. Japan Explos. Soc. **63**, 104 (2002).
[23] M. M. Kuklja, J. Phys. Chem. B **105**, 10159 (2001).
[24] S. Boyd, M. Gravelle, and P. Politzer, J. Chem. Phys. **124**, 104508 (2006).
[25] S. G. Boyd and K. J. Boyd, J. Chem. Phys. **129**, 134502 (2008).
[26] A. D. Buckingham, P. W. Fowler, and J. M. Hutton, Chem. Rev. (Washington, D.C.) **88**, 963 (1988).
[27] H. J. C. Berendsen, J. P. M. Postma, W. F. van Gunsteren, A. DiNola, and J. R. Haak, J. Chem. Phys. **81**, 3684 (1984).
[28] C. S. Choi and E. Prince, Acta Crystallogr. Sect. B: Struct. Crystallogr. Cryst. Chem. **28**, 2857 (1972).
[29] R. J. Karpowicz and T. B. Brill, J. Phys. Chem. **88**, 348 (1984).
[30] B. M. Rice and C. F. Chabalowski, J. Phys. Chem. A **101**, 8720 (1997).
[31] T. Vladimiroff and B. M. Rice, J. Phys. Chem. A **106**, 10437 (2002).
[32] M. M. Kuklja and B. B. Kunz, J. Phys. Chem. Solids **61**, 35 (2000).
[33] *LASL Explosive Property Data*, edited by T. R. Gibbs and A. Popolato (University of California Press, Berkeley, 1980).
[34] E. F. C. Byrd and B. M. Rice, J. Phys. Chem. A **110**, 1005 (2006).
[35] M. M. Kuklja and A. B. Kunz, J. Phys. Chem. B **103**, 8427 (1999).
[36] M. M. Kuklja, E. V. Stefanovich, and A. B. Kunz, J. Chem. Phys. **112**, 3417 (2000).